Optimal Combined Reaction-Wheel Momentum Management for LEO Earth-Pointing Satellites

Xiao-jiang Chen
Email: X.chen@ee.surrey.ac.uk
Tel: +44 1483 259278 ext. 3439

Willem H. Steyn
Email: H.steyn@ee.surrey.ac.uk
Tel: +44 1483 259278 ext. 3632

Center for Satellite Engineering Research (CSER), University of Surrey, Guildford, GU2 5XH, UK

Abstract: The optimal controllers for the management of 3-axis reaction-wheel momentum of rigid Earth-pointing satellites are analyzed in detail using magnetorquers and/or thrusters. Especially, two novel, optimal combined control schemes are proposed in order to achieve rapid, propellant-saving reaction wheel momentum dumping control by employing magnetorquers and thrusters. Finally, simulation results are presented to demonstrate the superiority of these algorithms. These two combined algorithms could easily be applied in real-time onboard an LEO Earth-pointing satellite.

I. Introduction

Earth-pointing satellites are expected to maintain the local-vertical/local-horizontal attitude in the presence of environmental disturbance effects.[1,3] Generally, this requires a spacecraft reaction wheel system to exchange momentum continuously with the spacecraft body. The secular external disturbance torques, for example, the torques due to passive gravity gradient, aerodynamic and solar forces, and active control torques from thrusters and magnetorquers, will tend to make the wheels drift toward saturation. Therefore, management of three-axis reaction wheel momentum is required in order to counteract the influence of persistent external disturbance torques. Usually an external torque must be applied, employing thrusters or magnetorquers, to force the wheel speed back to nearly zero momentum.

A number of relevant studies have been presented to cope with momentum dumping techniques. A cheap but slow unloading of RW momentum can be carried out by employing magnetorquers.[1, 2, 3] The effective and rapid momentum dumping can be achieved by thrusters at the cost of expendable propellant consumption.[4, 6] For satellites with thrusters, the minimization of thruster propellant dissipation is critically important to the space mission. In order to implement propellant-saving as well as rapid momentum dumping, we will discuss several combined control methods, simultaneously using 3-axis magnetorquers and thrusters to obtain a tradeoff between the dumping rate and propellant usage. So far there is no published paper addressing this application.

The paper is organized as follows: In Section II, we derive the general model of Earth-pointing RW momentum dumping. Then in Section III and IV the optimal LQR and minimum control energy (MEC) controllers using magnetorquers and PWM thrusters are described separately. Subsequently, in Section V the optimal combined control schemes are analyzed. In Section VI and VII the comparison of the control performance for different algorithms is shown.

II. Wheel Momentum Management Model of Rigid Satellites

The dynamic model of an Earth-pointing satellite using 3-axis reaction wheels as internal torque actuators and magnetorquers and thrusters as external torque actuators, and ignoring the small change of spacecraft inertia tensor due to thruster propellant consumption, is given by:

$$\mathbf{I}\dot{\omega}_{BY} = \mathbf{N}_T + \mathbf{N}_M + \mathbf{N}_{GG} + \mathbf{N}_D - \omega_{BY} \times (\mathbf{I}\omega_{BY} + \mathbf{h}) - \dot{\mathbf{h}} \quad (1)$$

where ω_{BY}, $\mathbf{I}$, $\mathbf{h}$, $\mathbf{N}_M$, $\mathbf{N}_T$, $\mathbf{N}_D$ and $\mathbf{N}_{GG}$ are respectively the inertially referenced body angular velocity vector, moment of inertia of spacecraft, three-axis reaction wheel angular momentum vector, applied torque vector by 3-axis magnetorquers, applied torque vector by 3-axis thrusters, external disturbance torque vector including the torques due to the aerodynamic and solar forces, and gravity gradient torque vector. We assume the satellite is 3-axis stabilized in a circular orbit, and then

$$\omega_{BY} = \omega_{LO} + \mathbf{T}_{BYLO}\,\omega_0 \qquad (2)$$

where ω_{LO} is body angular rate with respect to the local orbital coordinates, and

$$\mathbf{T}_{BYLO} = \begin{bmatrix} A_{11} & A_{12} & A_{13} \\ A_{21} & A_{22} & A_{23} \\ A_{31} & A_{32} & A_{33} \end{bmatrix}$$

is the attitude matrix from local orbital to body coordinates,

$$\omega_0 = \begin{bmatrix} 0 & -\omega_0 & 0 \end{bmatrix}^T$$

constant orbital angular rate vector.

If we assume a fixed Earth-pointing attitude with nadir or off-nadir pointing, we have:

$$\omega_{LO} = \begin{bmatrix} \omega_{ox} & \omega_{oy} & \omega_{oz} \end{bmatrix}^T = \begin{bmatrix} 0 & 0 & 0 \end{bmatrix}^T$$

$\mathbf{T}_{BYLO}$ = constant attitude matrix

$\mathbf{N}_{GG}$ = constant vector

Furthermore, we define

$$\mathbf{N}_{con} = -\omega_{BY} \times \mathbf{I}\omega_{BY} + \mathbf{N}_{GG} = \text{constant vector} \qquad (3)$$

The magnetic torque vector $\mathbf{N}_M$ can be written as the cross-product of the magnetic dipole moment $\mathbf{M}$ of the magnetic coils with the measured magnetic field strength $\mathbf{B}$ in body frames by 3-axis magnetometers:

$$\mathbf{N}_M = \mathbf{M} \times \mathbf{B} = \mathbf{Q}(t)\mathbf{M} \qquad (4)$$

where $\mathbf{M}$ is magnetic dipole control moment vector, and

$$\mathbf{Q}(t) = \begin{bmatrix} 0 & B_z(t) & -B_y(t) \\ -B_z(t) & 0 & B_x(t) \\ B_y(t) & -B_x(t) & 0 \end{bmatrix} \qquad (5)$$

The measured magnetic field $\mathbf{B}$ can be given by:

$$\mathbf{B} = \mathbf{T}_{BYLO}\,\mathbf{B}_o \qquad (6)$$

where $\mathbf{B}_o$ is geomagnetic field vector in the local orbital coordinates. Therefore, the reaction wheel momentum desaturation model with a fixed Earth-pointing attitude in a circular orbit can be represented as (ignoring the weak effect of the small external disturbance torque $\mathbf{N}_D$):

$$\dot{\mathbf{h}}(t) = \mathbf{W}\mathbf{h}(t) + \left[\mathbf{N}_T + \mathbf{Q}(t)\mathbf{M} + \mathbf{N}_{con}\right] \qquad (7)$$

with,

$$\mathbf{W} = \begin{bmatrix} 0 & -\omega_o A_{32} & \omega_o A_{22} \\ \omega_o A_{32} & 0 & -\omega_o A_{12} \\ -\omega_o A_{22} & \omega_o A_{12} & 0 \end{bmatrix} = \text{constant matrix}$$

Accordingly, Eq. (7) can be regarded as the general model for the management of three-axis reaction wheel momentum on Earth-pointing satellites. This model implies that, only if the torques generated by 3-axis reaction wheel are equal to the sum of the satellite gyroscopic torques, active torque by 3-axis magnetorquers, cold-gas thrusters and external disturbances, the satellite will keep the fixed required Earth-pointing attitude and the RW momentum can be managed by external torques to the expected values.

For the perfect nadir-pointing case ($\mathbf{N}_{con} = \mathbf{0}$), the RW momentum dumping model could be simplified by: (Steyn[3])

$$\dot{\mathbf{h}}(t) = \mathbf{W}\mathbf{h}(t) + \left[\mathbf{N}_T + \mathbf{Q}(t)\mathbf{M}\right] \qquad (8)$$

where,

$$\mathbf{W} = \begin{bmatrix} 0 & 0 & \omega_o \\ 0 & 0 & 0 \\ -\omega_o & 0 & 0 \end{bmatrix} \qquad (9)$$

III. Optimal Desaturation Controllers using Magnetorquers

A. Linear Quadratic Controllers (LQR and ILQR)

Steyn[3] in his thesis has developed several optimal desaturation algorithms using 3-axis magnetorquers for the perfect nadir-pointing case in Eq.

(8). Here, an optimal feedback control law to regulate the wheel momentum vector **h** towards the zero vector for the general model in Eq. (7) is to be derived by minimizing the following cost function:

$$J = \frac{1}{2}\int_{t_0}^{t_f} \{\mathbf{h}^T\mathbf{F}\mathbf{h} + \mathbf{M}^T\mathbf{R}\mathbf{M}\}\, dt \qquad (10)$$

where t_0, t_f are the initial and final time, **F** is a non-negative symmetric weighting 3-by-3 matrix for the wheel angular momentum, and **R** is a positive symmetric weighting 3-by-3 matrix for the magnetic coil moments. According to the Pontryagin's principle of optimal theory, we can get the control equation:

$$\mathbf{M}(t) = -\mathbf{R}^{-1}\mathbf{Q}^T(t)[\mathbf{K}(t)\mathbf{h} - \mathbf{g}(t)] \qquad (11)$$

where $\mathbf{K}(t)$ is a time-dependent 3-by-3 gain matrix, and $\mathbf{g}(t)$ is a time-dependent 3-by-1 vector. They are solved by the backwards integration of a two-point boundary value problem. The values of $\mathbf{K}(t)$ and $\mathbf{g}(t)$ at sampled intervals can then be stored in an onboard look-up table to be used at the corresponding orbital locations for desaturation control.

As an alternative, a fairly accurate quasi-static LQR feedback control law can be computed by an on-line solution of the infinite time LQR (ILQR) control problem at every sample time.[3] This method explores the slowly varying nature of the geomagnetic field. This alternative method is computational demanding because the eigenvector decomposition of a six-order Hamiltonian matrix must be done every sample time. But no large look-up tables are needed compared to the standard LQR method.

B. Minimum-Energy Controller (MEC)

Another fixed terminating time, minimum-energy, optimal controller was presented[3] by minimizing the cost function subject to the constraint of Eq. (7) without the terms of $\mathbf{N}_T$:

$$J = \frac{1}{2}\int_{t_0}^{t_f} \mathbf{M}^T\mathbf{M}\, dt \qquad (12)$$

The optimal control can be obtained as:

$$\mathbf{M}(t) = -\mathbf{Q}^T(t)e^{\mathbf{W}t}\mathbf{p}(t_0) \qquad (13)$$

Substitute Eq. (13) into Eq. (7) (without the term $\mathbf{N}_T$), then

$$\dot{\mathbf{h}}(t) = \mathbf{W}\mathbf{h}(t) - \mathbf{Q}(t)\mathbf{Q}^T(t)e^{\mathbf{W}t}\mathbf{p}(t_0) + \mathbf{N}_{con} \qquad (14)$$

The variation of extremals method[3] can now be used to solve $\mathbf{p}(t_0)$.

The MEC optimal control moment $\mathbf{M}(t)$ depends on the solution of $\mathbf{p}(t_0)$, and this can be done off-line for a specific orbit window. Note that the MEC controller will completely work in open-loop as the solution for $\mathbf{M}(t)$ does not make use of any wheel momentum measurements.

C. Summary

Both the LQR and MEC controller addressed above can be applied to achieve optimal wheel momentum desaturation using three-axis magnetorquers. However, both these methods finally have to resort to solving the two-point boundary value problem[3] based upon the knowledge of the local geomagnetic field and require the amplitude of the moment of magnetic coils to be unbounded. The feedback nature of the LQR controllers would be preferred. The LQR controllers will ensure robustness against modeling errors and external disturbances. If the geomagnetic field does not change much between successive orbits, an orbital LQR gain lookup table can be calculated off-line and then used onboard. The MEC controllers will consume the least amount of energy as expected. However, due to their open-loop nature and non-ideal off-line calculations when solving the boundary value problem, such as modeling errors (e.g. geomagnetic field) and external torque disturbances on the stabilized satellite, their control accuracy is limited.[3]

IV. Optimal Desaturation Controllers using PWM Thrusters

The thrusters could be employed to implement a relatively rapid management of the wheel momentum compared with magnetorquers. If the thrusters are used in the PWM mode, they can be approximated as linear actuators. The model of Eq. (7) in this case can be simplified as:

$$\dot{\mathbf{h}}(t) = \mathbf{W}\mathbf{h}(t) + \mathbf{N}_T + \mathbf{N}_{con} \qquad (15)$$

A. Linear Quadratic Controllers (LQR and ILQR)

Similarly, the optimal feedback control law to regulate the wheel momentum vector **h** towards the zero vector, using PWM thrusters, is derived by minimizing the following cost function:

$$J = \frac{1}{2}\int_{t_0}^{t_f} \{\mathbf{h}^T\mathbf{F}\mathbf{h} + \mathbf{N}_T{}^T\mathbf{R}\mathbf{N}_T\}\, dt \qquad (16)$$

Similarly, the optimal control law is given by:

$$\mathbf{N}_T(t) = -\mathbf{R}^{-1}\mathbf{K}(t)\mathbf{h}(t) + \mathbf{R}^{-1}\mathbf{g}(t) \qquad (17)$$

The time-dependent 3-by-3 gain matrix $\mathbf{K}(t)$ and 3-by-1 vector $\mathbf{g}(t)$ can be saved in look-up tables to achieve on-board optimal desaturation control using PWM thrusters. If the infinite time LQR (ILQR) is adapted, the constant gain matrix $\mathbf{K}_\infty$ and vector $\mathbf{g}_\infty$ can be used. Due to the time invariance of the wheel momentum management model in Eq. (15), there is no need to build up the look-up gains in on-board memory or to solve the ILQR problem every sampling period. The gain matrix $\mathbf{K}_\infty$ and vector $\mathbf{g}_\infty$, due to the choice of the weighting matrixes **R** and **F**, will determine the final response time of the desaturation system.

B. Minimum-Energy Controller (MEC)

A fixed terminal time, minimum-energy optimal controller can be derived by minimizing the energy cost function subject to the constraint of Eq. (15):

$$J = \frac{1}{2}\int_{t_0}^{t_f} \mathbf{N}_T{}^T\mathbf{N}_T\, dt \qquad (18)$$

In the same way, the optimal control torque will be:

$$\mathbf{N}_T(t) = -e^{\mathbf{W}'}\mathbf{p}(t_0) \qquad (19)$$

Similarly, the initial state vector $\mathbf{p}(t_0)$ in Eq. (19) can be solved off-line as in Section III. Thereby, the optimal minimum-energy control (MEC) torque $\mathbf{N}_T(t)$ with the open-loop nature using PWM thrusters is obtained.

V. Combined Desaturation Controllers using Magnetorquers and PWM Thrusters

Magnetorquers and thrusters respectively have their own advantages and disadvantages for 3-axis reaction wheel momentum management as shown in Table 1.

Saving the thruster propellant is significant for an attitude control system equipped with thrusters. The authors have not found any papers that deal with the combined management of reaction wheel momentum using magnetorquers and thrusters simultaneously. Next, we shall present an optimal combined control algorithm, and a combined control algorithm using a cross-product law, which make full use of the advantages of magnetorquers and thrusters. The algorithms are simple and suitable for on-board real-time applications.

Table1 Comparison of magnetorquers and thrusters for RW momentum dumping

Actuator	Advantage	Disadvantage
Magnetorquers	• Do not generate translational forces, therefore do not perturb the orbit • Do not consume any thruster propellant	• The produced torque is relatively small, thus the momentum dumping rate is slow
Thrusters	• Can achieve rapid momentum dumping and remove much more momentum in a given period of time	• Consume expendable propellant • Can generate translational forces to influence the satellite's orbit

A. Optimal Combined Desaturation Controllers (OCDC)

The optimal LQR, ILQR and MEC controllers for PWM control of thrusters discussed above can be used to obtain the dumping torque during a fixed time period from t_0 to t_f. If we want the torque $\mathbf{N}(k)$ at every sample time to be generated simultaneously by magnetorquers and PWM thrusters, we can define:

$$\mathbf{N}(k) = \mathbf{N}_T(k) + \mathbf{Q}(k)\mathbf{M}(k) \qquad (20)$$

where $\mathbf{N}_T(k)$ is 3-axis PWM thruster torque, and $\mathbf{Q}(k)$ defined in Eq. (5). Reorganize Eq. (20) as:

$$\mathbf{N}(k) = \mathbf{A}(k)\mathbf{N}_{MT}(k) \qquad (21)$$

where,

$$\mathbf{A}(k) = \begin{bmatrix} 0 & B_z(k) & -B_y(k) & 1 & 0 & 0 \\ -B_z(k) & 0 & B_x(k) & 0 & 1 & 0 \\ B_y(k) & -B_x(k) & 0 & 0 & 0 & 1 \end{bmatrix}$$

$$\mathbf{N}_{MT}(k) = \left[M_x(k)\ M_y(k)\ M_z(k)\ N_{Tx}(k)\ N_{Ty}(k)\ N_{Tz}(k) \right]^T$$

In order to arrive at the formulation of an optimal combined controller, the following cost function is proposed:

$$J = \frac{1}{2}\mathbf{N}_{MT}^T(k)\mathbf{S}\mathbf{N}_{MT}(k) + \lambda^T\left[\mathbf{N}(k) - \mathbf{A}(k)\mathbf{N}_{MT}(k)\right] \quad (22)$$

where λ is a 3-by-1 vector of Lagrange multipliers that adjoin the constant equations to the scalar cost equation, and **S** is a 6-by-6 constant positive weighting matrix. We define **S** to be a diagonal positive matrix having the form:

$$\mathbf{S} = \mathrm{diag}(a, a, a, b, b, b)$$

where a and b are positive scalars. In order to minimize J, we take derivatives of Eq. (22) with respect to $\mathbf{N}_{MT}$ and λ giving the two vector equations:

$$\mathbf{N}(k) = \mathbf{A}(k)\mathbf{N}_{MT}(k) \quad (23\text{-a})$$

$$\mathbf{N}_{MT}(k) = \mathbf{S}^{-1}\mathbf{A}^T(k)\lambda \quad (23\text{-b})$$

Solving for $\mathbf{N}_{MT}$,

$$\mathbf{N}_{MT}(k) = \mathbf{S}^{-1}\mathbf{A}^T(k)\left[\mathbf{A}(k)\mathbf{S}^{-1}\mathbf{A}^T(k)\right]^{-1}\mathbf{N}(k) \quad (24)$$

Eq. (24) is the optimal blending algorithm for magnetorquers and thrusters during wheel momentum management. This equation divides the required torque $\mathbf{N}(k)$ optimally into two parts. One part has to be generated by the magnetorquers and the other part by the PWM thrusters. The supporting torques produced by the magnetorquers could obviously reduce the consumption of the limited thruster propellant.

B. Combined Desaturation Controllers using a Cross-Product Law

The conventional well-known magnetorquing cross-product control[2, 3] is given by :

$$\mathbf{M} = -k(\mathbf{N} \times \mathbf{B})/\|\mathbf{B}\| \quad (25)$$

where **M** is regarded as the most favorable magnetorquing vector, **B** is the body geomagnetic field vector measured by on-board magnetometers, **N** is the required control torque vector and k is a constant scalar gain.

The active magnetic torque $\mathbf{N}_M$ must be in the plane P_B normal to the vector **B** shown in Fig. 1. We propose that the best torque $\mathbf{N}_M$ is one which is the projection of the desired **N** in plane P_B. This will be the minimum error condition. As a result, the desired $\mathbf{N}_M$ has the smallest error with respect to **N**. The common cross-product in Eq. (25) could not achieve this as it only ensures the correct vector direction for $\mathbf{N}_M$ but the magnitude of $\mathbf{N}_M$ will still depend on the scalar gain k. Therefore, if we wish to minimize the error between **N** and $\mathbf{N}_M$, the cross-product law could be revised as:

$$\mathbf{M} = -(\mathbf{N} \times \mathbf{B})/\|\mathbf{B}\|^2 \quad (26)$$

where the correct value for the scalar gain k is inversely proportional to the magnetic field magnitude. According to the cross product law in Eq. (26), the active magnetic torque vector $\mathbf{N}_M$ generated by magnetorquers is the projection of **N** in plane P_B in Fig. 1.

$$\mathbf{N}_M = \mathbf{M} \times \mathbf{B} = N \sin\beta \cdot (\hat{\mathbf{M}} \times \hat{\mathbf{B}}) \quad (27)$$

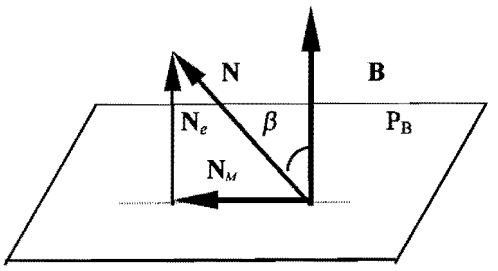

Fig. 1 The configuration of the favorable torque generated by magnetorquer

where N is the amplitude of the required torque vector **N**, $\hat{\mathbf{M}}$ and $\hat{\mathbf{B}}$ are the unit vectors of **M** and **B**, and β is the angle between the vectors **N** and **B**.

Based upon the revised cross-product law for magnetorquer control, the combined controller for the management of reaction-wheel momentum is derived by:

$$\mathbf{N}(k) = \mathbf{N}_T(k) + \mathbf{N}_M(k) \quad (28)$$

where $\mathbf{N}_M(k)$ is the favorable torque by magnetorquers in Eq.(28). Therefore, $\mathbf{N}_T(k)$ must be equal to the torque error $\mathbf{N}_e$ in Fig. 1, which has the

minimum amplitude. Additionally, the amplitudes of vector $\mathbf{N}(k)$ and $\mathbf{N}_T(k)$ satisfies the following relation:

$$N(k) \geq N_T(k) \qquad (29)$$

Eq. (29) ensures that the PWM thrusters will minimize the fuel control energy during the combined management of the 3-axis RW momentum.

VI. Comparison of the Controllers

Simulations were implemented to investigate the performance of all the RW momentum dumping controllers analyzed above. The satellite UoSAT-12 is used as an example during these simulations. The proposed methods will also be suitable for satellites in other operating conditions. UoSAT-12 is the first low-cost LEO mini-satellite with 3-axis earth-pointing capability built by Surrey Space Center and equipped with 3-axis reaction wheels, magnetorquers and cold-gas thrusters. It is expected to be launched in a 650km sun-synchronous circular orbit by early 1999. Its orbital period is nearly 100 minutes.

The Earth's magnetic field is simply defined as a first dipole model during simulations. In the local orbital coordinates, the model for UoSAT-12 could be expressed as:[3, 4]

$$\mathbf{B}_o = \begin{bmatrix} B_{ox} \\ B_{oy} \\ B_{oz} \end{bmatrix} \approx \begin{bmatrix} 23\cos\omega_o t \\ 2.4 \\ 46\sin\omega_o t \end{bmatrix} \mu T \qquad (30)$$

During the simulations we assumed that both the cold-gas thrusters work in PWM mode with a minimum firing time of 50 milli-seconds each. The thruster torque has a constant value of ±40 milli-Nm during the active firing period. In addition, we assume the magnetic moment to be unbounded, and the sample time to be 10 seconds. A perfect nadir-pointing attitude i.e. $\mathbf{N}_{con} = \mathbf{0}$ in Eq. (7) is also assumed during simulations.

A. Simulations of Optimal Dumping Controllers using Magnetorquers

The proposed optimal controllers LQR, ILQR and MEC using magnetorquers are compared with a common cross-product law (CCPL) dumping algorithm:

$$\mathbf{M} = K_m(\mathbf{h} \times \mathbf{B})/\|\mathbf{B}\| \qquad (31)$$

where K_m is a scalar gain. In order to evaluate the performance of every controller, a control energy function for magnetic control moment $\mathbf{M}$ is defined as:[1]

$$J_M(t) = \frac{1}{2}\int_{t_0}^{t} \mathbf{M}^T\mathbf{M}\, dt \qquad t_0 \leq t \leq t_f \qquad (32)$$

Fig. 2 shows a half-orbit (3000-second) momentum dumping effort using the magnetorquer ILQR, LQR, MEC and CCPL controllers (For clarity only, the momentum amplitude $\|\mathbf{h}\|$ is shown). We can see the MEC controller consumes the least energy, and the energy cost of CCPL is the highest.

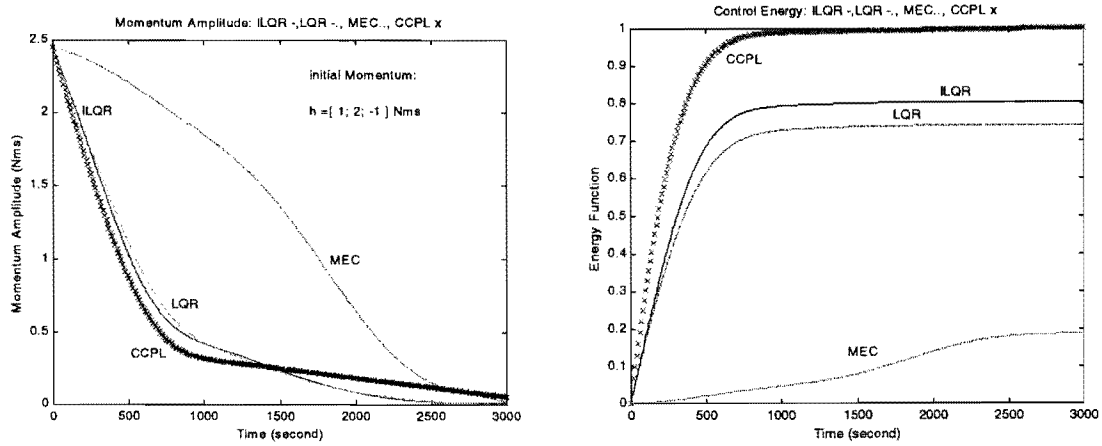

Fig. 2 RW momentum dumping using magnetorquers only *

* *Note: All the energy cost investigations shown in the figures and tables are normalized w.r.t. the maximum value*

B. Simulation of Dumping Controllers using Thrusters only and Combined Methods

Similarly the energy function for PWM cold-gas thrusters is also introduced:

$$J_{N_T}(t) = \frac{1}{2}\int_{t_0}^{t} \mathbf{N}_T{}^T \mathbf{N}_T \, dt \qquad t_0 \le t \le t_f \quad (33)$$

Furthermore, the accumulated firing time of thrusters is investigated to asses the fuel consumption. Based upon the optimal controllers LQR, ILQR and MEC using PWM cold-gas thrusters (CT), the combined dumping algorithms, including the optimal combined algorithm (OCDC), the combined algorithms using the conventional cross-product law (CCCP) and revised cross-product law (CRCP), were simulated and compared to the dumping controller using thrusters only (DCT).

Fig. 3 and 4 respectively show an one-tenth-orbit (600-second) momentum dumping effort using thrusters only and their combined methods based upon the ILQR, LQR and MEC controllers. Table 2 list the overall results from the viewpoint of the propellant consumption and magnetorquer (MT) control energy cost for an one-tenth-orbit momentum dumping effort.

The simulations show that the dumping performance of the controllers stays unchanged. When using thrusters only (DCT), the behavior of ILQR is almost the same as LQR. MEC consumes the least amount of control energy, but its accumulated firing time is still almost similar to that of LQR. In addition, the combined method (CRCP) generally consumes the least amount of thruster propellant. The optimal combined controller (OCDC) in Eq. (24) tends to have the same effect as CRCP when the weighting matrix **S** has weight a as positively infinitesimal and weight b as positively infinite. This phenomenon can be explained by Fig. 1. For the optimal combined controller (OCDC) in Eq. (24), to minimize the cost function in Eq. (22), it requires that the weighting component a approaches positive infinitesimal and b positive infinite. Then the thruster control vector $\mathbf{N}_T(k)$ will tend to be vector $\mathbf{N}_e$ in Fig. 1, which ensures the minimum-amplitude error between $\mathbf{N}$ and $\mathbf{N}_M$. Therefore, CRCP and OCDC could be the favored controllers for combined momentum dumping of magnetorquers and thrusters. In practice, CRCP will need less processing time. Furthermore, CCCP will consume the most magnetic control energy. OCDC could balance the magnetic control energy cost and thruster fuel consumption by changing the weighting matrix **S**.

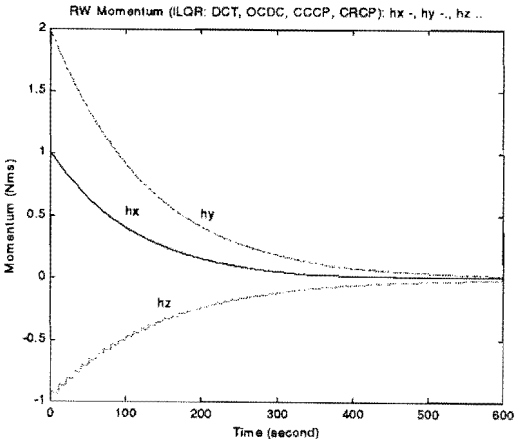

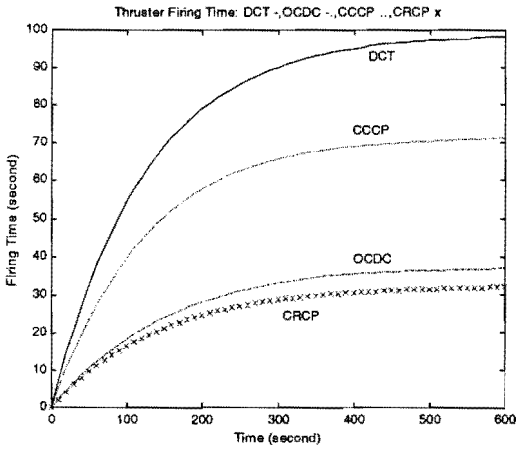

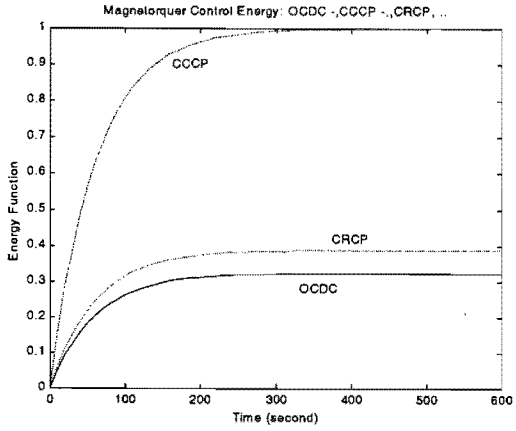

Fig. 3 RW momentum dumping using thrusters only and combined methods based upon the LQR, ILQR controllers

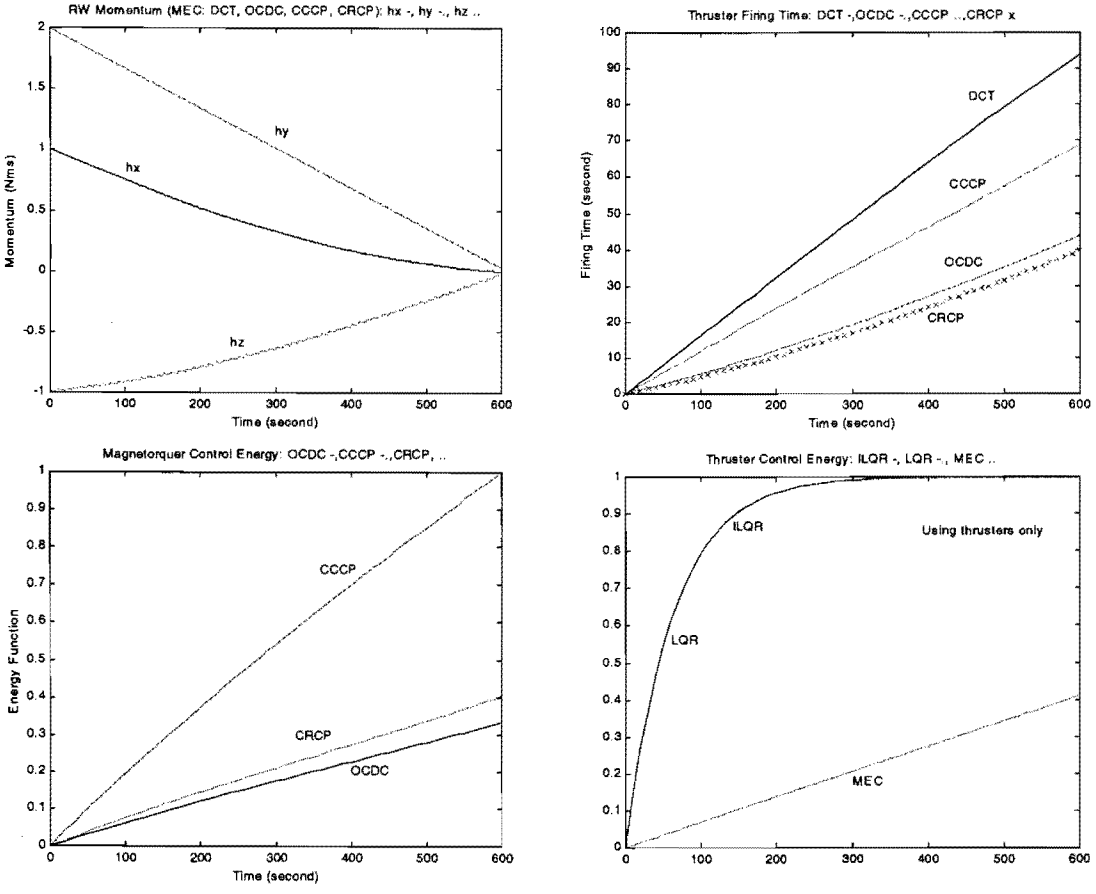

Fig. 4 RW momentum dumping using thrusters only and combined methods based upon the MEC controllers and thruster control energy comparison for DCT

Table 2 The comparison of the combined controllers

Dumping methods	ILQR (0.1 orbit, 600 seconds)			MEC (0.1 orbit, 600 seconds)		
Initial momentum (Nms)	[1;2; -1]	[2;-1.2;0.5]	[1.2;-0.8;-2]	[1; 2; -1]	[2; -1.2; 0.5]	[1.2;-0.8; -2]
Starting point from ascending node (orbit)	0.23	0.56	0.67	0.23	0.56	0.67
DCT						
CT firing time(sec)	98.25	87.75	95.30	93.90	88.15	89.35
CCCP						
• CT firing time(sec)	71.25	53.75	74.35	68.70	42.65	74.80
• Fuel-saving (%)	27.48	38.77	21.97	26.83	51.61	16.27
• MT energy cost	1.00	1.00	1.00	1.00	1.00	1.00
CRCP						
• CT firing time(sec)	31.95	52.80	56.00	39.50	31.35	50.75
• Fuel-saving (%)	67.48	39.83	41.23	57.93	64.43	43.21
• MT energy cost	0.39	0.88	0.45	0.61	0.69	0.42
OCDC						
• CT firing time(sec)	36.90	53.30	57.20	43.55	34.75	60.85
• Fuel-saving (%)	62.44	39.24	40.00	53.62	60.59	31.88
• MT energy cost	0.33	0.63	0.37	0.21	0.50	0.35

VII. Discussion of Results

To summarize, combined reaction wheel momentum dumping algorithms were developed using an optimal combined controller (OCDC) and a revised cross-product law (CRCP). The combined controllers OCDC and CRCP just rely on the measured geomagnetic field B(k) and resort to a predetermined torque vector $\mathbf{N}(k)$, as calculated by the optimal LQR, ILQR or MEC method in Section IV. However, the beneficial point is that the required control torque $\mathbf{N}(k)$ for dumping wheel momentum has been generated by an optimized blending of both magnetorquers and PWM cold-gas thrusters. This means that thruster propellant can be saved due to the assistance of the magnetorquers. Importantly, there is no need to predict off-line the local geomagnetic field vector for these combined controllers. The magnetic field is simply obtained by magnetometer measurements. The control blending of the magnetorquers and thrusters can be computed simply from Eq. (24) or (28). Therefore, the combined controllers discussed above can be adapted to practically achieve rapid, propellant-saving optimal management of the 3-axis reaction-wheel momentum during the expected time period from t_0 to t_f.

However, all these theoretical analyses assume that the magnetorquer control value to be unbounded and continuous. In practice, the firing of magnetorquers can not be allowed during the period of magnetometer measurements and the magnetorquers also have a saturation limit. This saturation limit for these combined algorithms (OCDC and CRCP) has a considerable effect. For UoSAT-12, the maximum magnetic dipole moment along every axis is nearly 40 Am^2. In order to model this saturation effect, we can add the following conditions to the simulation. If any component of $\mathbf{M}(k)=\left[M_x(k) \quad M_y(k) \quad M_z(k)\right]^T$ calculated from Eq.(24) or (28) exceeds the limit value, we can compensate the thruster control logic as follows:

$$\Delta\mathbf{N}_T(k) = \mathbf{Q}(k)[\mathbf{M}(k) - \mathbf{M}_{\max}] \qquad (34)$$

where $\Delta\mathbf{N}_T(k)$ is the thruster compensated control vector, and $\mathbf{M}_{\max}$ is the saturation value of magnetic moment. The thrusters also compensate for the lack of available magnetic torque.

The simulations of momentum management for the UoSAT-12 mission were repeated with the saturation constraint added, to check the feasibility and expected performance of the combined optimal controller OCDC. During the simulations we assumed that magnetorquers also work in PWM mode with a minimum firing time of 50 milli-seconds each. The maximum firing time period is 9 seconds per sample time of 10 seconds. Fig. 5 and 6 just show a comparison of thruster and magnetorquer activities for the combined method OCDC and for thruster only (DCT) during an one-tenth-orbit (600-second) reaction wheel momentum dumping effort. The momentum

dumping behavior is same as in Fig. 3 and 4. Table 3 lists several representative simulation results. Due to a variation of the geomagnetic field in orbit at different start positions during simulation, the thruster firing saving time will be different over similar dumping periods. However, the simulations show that the combined momentum dumping method can definitely save a large amount of thruster propellant.

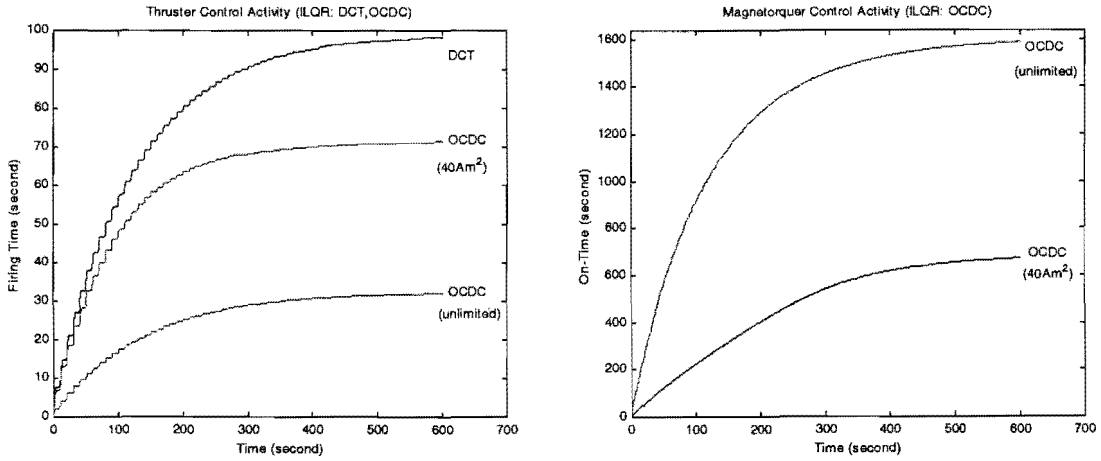

Fig. 5 UoSAT-12 RW momentum dumping using thrusters only and combined method OCDC based upon the ILQR controller

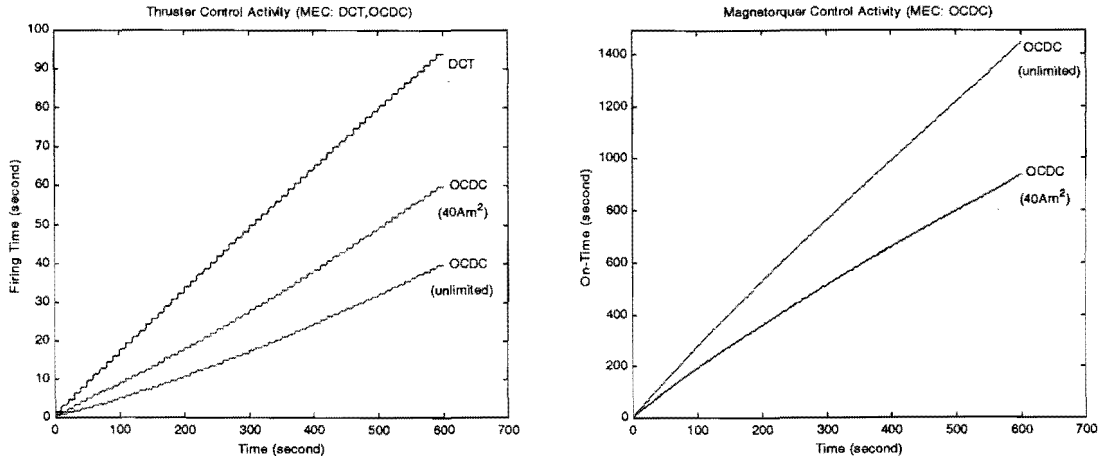

Fig. 6 UoSAT-12 RW momentum dumping using thrusters only and combined method OCDC based upon the MEC controller

Table 3 RW momentum dumping using OCDC and thruster only (DCT) for UoSAT-12

Dumping methods	ILQR (0.1 orbit, 600 seconds)			MEC (0.1 orbit, 600 seconds)		
Initial momentum (Nms)	[1;2; -1]	[2;-1.2;0.5]	[1.2;-0.8;-2]	[1; 2; -1]	[2; -1.2; 0.5]	[1.2;-0.8; -2]
Starting point from ascending node (orbit)	0.23	0.56	0.67	0.23	0.56	0.67
DCT CT firing time(sec)	98.25	87.75	95.30	93.90	88.15	89.35
OCDC						
• CT firing time(sec)	71.45	68.55	73.00	59.90	48.15	59.40
• Fuel-saving (%)	27.28	21.88	23.40	36.21	44.64	33.52

VIII. Conclusions

The wheel momentum buildup due to secular disturbances must be reduced by actively applying compensating external torques of both 3-axis magnetorquers and cold-gas thrusters. The optimal LQR, and MEC controllers discussed in this paper can be applied to achieve wheel momentum desaturation using three-axis magnetorquers and PWM thrusters separately. The LQR controllers is preferred due to their feedback nature. These controllers will ensure robustness against modeling errors and external disturbances. The MEC controllers will consume the least amount of energy. However, due to their open-loop nature and non-ideal simulation conditions, such as modeling errors (e.g. geomagnetic field, and the change of spacecraft inertia tensor due to thruster propellant consumption) and external torque disturbances on the stabilized satellite, their control accuracy is limited.[7] The optimal controllers using magnetorquers only, strongly depend on the geomagnetic field model. If the complicated IGRF model is employed, a great computation effort is required to solve the two-point boundary problem for on-board applications.

The newly proposed combined dumping controllers exploit the merits of both magnetorquers and PWM thrusters. Based upon relatively simple thruster optimal algorithms, the blending methods effectively separate the required torques for magnetorquer and thruster commanding. They do not require geomagnetic field estimations, but employ on-line magnetometer measurement data. Therefore, they could be suitable in practice for achieving rapid, propellant-saving 3-axis reaction wheel momentum dumping. Simulation results have been given to illustrate the merits of the proposed combined algorithms. The expected performance of these controllers were obtained.

Acknowledgments

The authors wish to acknowledge the support given by Prof. Martin Sweeting and the Surrey Space Center ADCS team.

Reference

1. Hiroshi, I. and N. Keiken, "A New Approach to Magnetic Angular Momentum Management for Large Scientific Satellites", NEC Research & Development, Vol. 37, No.1, January 1996, pp. 60-77.
2. Chang, D.H., "Magnetic and Momentum Bias Attitude Control Design for the HETE Small Satellite", Proceedings of the 6th AIAA/USU Conference on Small Satellites, Utah State University, Sept. 1992.
3. Steyn, W.H., "Chapter 4. Momentum Dumping", A Multi-mode Attitude Determination and Control System for Small Satellites, PhD thesis, University of Stellenbosch, December 1995.
4. Wertz, J.R., Spacecraft Attitude Determination and Control, D. Reidel Publishing Company, Dordrecht, Holland, 1989.
5. Bshrivastava, S.K. and V.J. Modi, "Satellite Attitude Dynamics and Control in the Presence of Environmental Torques—A Brief Survey", Journal of Guidance, Control and Dynamics, Vol. 6, No.6, Nov.-Dec. 1983, pp. 461-471.
6. Creamer, G., P. DelaHunt and S. Gates, "Attitude Determination and Control Clementine during Lunar Mapping", Journal of Guidance, Control and Dynamics, Vol. 19, No.3, May-June 1996, pp. 505-511.